Article

# Comparative Photophysics of [26]- and [28]Hexaphyrins(1.1.1.1.1.1): Large Two-Photon Absorption Cross Section of Aromatic [26]Hexaphyrins(1.1.1.1.1.1)

Tae Kyu Ahn, Jung Ho Kwon, Deok Yun Kim, Dae Won Cho, Dae Hong Jeong, Seong Keun Kim, Masaaki Suzuki, Soji Shimizu, Atsuhiro Osuka, and Dongho Kim

*J. Am. Chem. Soc.*, **2005**, 127 (37), 12856-12861• DOI: 10.1021/ja050895l • Publication Date (Web): 27 August 2005



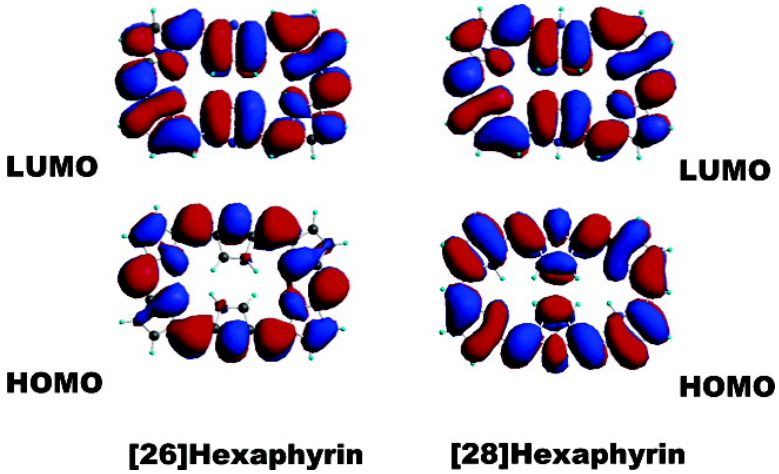


## More About This Article

Additional resources and features associated with this article are available within the HTML version:

- Supporting Information
- Links to the 22 articles that cite this article, as of the time of this article download
- Access to high resolution figures
- Links to articles and content related to this article
- Copyright permission to reproduce figures and/or text from this article

View the Full Text HTML

J|A|C|S
ARTICLES
Published on Web 08/27/2005

# Comparative Photophysics of [26]- and [28]Hexaphyrins(1.1.1.1.1.1): Large Two-Photon Absorption Cross Section of Aromatic [26]Hexaphyrins(1.1.1.1.1.1)

Tae Kyu Ahn,[†,||] Jung Ho Kwon,[†] Deok Yun Kim,[†] Dae Won Cho,[‡] Dae Hong Jeong,[§] Seong Keun Kim,[||] Masaaki Suzuki,[⊥] Soji Shimizu,[⊥] Atsuhiro Osuka,*[,⊥] and Dongho Kim*[,†]

*Contribution from the Center for Ultrafast Optical Characteristics Control and Department of Chemistry, Yonsei University, Seoul 120-749, Korea, Department of Chemistry, Seonam University, Namwon 590-711, Korea, Department of Chemistry Education and Nano-Systems Institute (NSI-NCRC), and School of Chemistry, Seoul National University, Seoul 151-747, Korea, and Department of Chemistry, Graduate School of Science CREST of JST, Kyoto University, Kyoto 606-8502, Japan*

Received February 11, 2005; E-mail: osuka@kuchem.kyoto-u.ac.jp; dongho@yonsei.ac.kr

***Abstract:*** We have explored the electronic natures of representative expanded porphyrins, [26]- and [28]-hexaphyrins, to investigate the interplay between the aromaticity and antiaromaticity that is brought by two electron oxidation/reduction processes. The excited singlet and triplet states of [26]hexaphyrin in solution exhibit lifetimes of 125 ps and 1.8 $\mu$s, respectively, as revealed by various time-resolved spectroscopic measurements. On the other hand, [28]hexaphyrin shows faster singlet and triplet lifetimes than those of [26]hexaphyrin, which is largely in accordance with the perturbation of aromaticity due to the $\pi$ electron formulation of [4$n$] in [28]hexaphyrins. The two-photon absorption cross-section values at 1200 nm for [26]hexaphyrins show ca. 9890 GM which is $>10^2$ larger than those of porphyrins. The reduced TPA values of 2600 and 810 GM of [28]hexaphyrin and perfluorinated [28]hexaphyrin, respectively, match well with their relatively short excited-state lifetimes. Overall, the enhanced excited-state lifetimes for various hexaphyrins go in line with the increased TPA cross-section values and the ring planarity.

## Introduction

Recently, expanded porphyrins with more than four pyrrole subunits in the porphyrin macrocycle have emerged as a promising class of molecules in light of versatilities in their optical, electrochemical, and coordination properties.[1−5] Because of an increased $\pi$ conjugation pathway, the electronic structures of expanded porphyrins give rise to considerably red-shifted HOMO−LUMO transitions relative to those of porphyrins. Numerous kinds of expanded porphyrins have so far been prepared by taking advantage of the flexibilities in connecting pyrrole rings, overall structures, and heteroatom substitution on pyrrole nitrogens. Despite the synthetic diversity of expanded porphyrins, their characterizations are mainly limited to the structural analyses such as $^1$H NMR and X-ray, along with some absorption spectra.[6] In this regard, it is relevant to investigate the photophysical properties of representative expanded porphyrins [26] and [28]hexaphyrins(1.1.1.1.1.1) to provide a platform for further investigations on the electronic structures of a series of expanded porphyrins.

[26]Hexaphyrins(1.1.1.1.1.1) and [28]hexaphyrins(1.1.1.1.1.1) are attractive molecules in view of aromaticity/antiaromaticity with a 26/28$\pi$-electronic circuit, intense UV-absorption, a small

[†] Yonsei University.
[‡] Seonam University.
[§] Department of Chemistry Education and Nano-Systems Institute, Seoul National University.
[||] School of Chemistry, Seoul National University.
[⊥] Kyoto University.

(1) (a) Strickler, J. H.; Webb, W. W. *Opt. Commun.* **1991**, *16*, 1780. (b) Kawata, S.; Sun, H.-B.; Tanaka, T.; Takada, K. *Nature* **1999**, *398*, 697.
(2) (a) Anderson, H. L.; Martin, S. J.; Bradleu, D. D. C. *Angew. Chem., Int. Ed. Engl.* **1994**, *33*, 655. (b) Screen, T. E. O.; Throne, J. R. G.; Denning, R. G.; Bucknall, D. G.; Anderson, H. L. *J. Am. Chem. Soc.* **2002**, *124*, 9712. (c) LeCours, S. M.; Guan, H.-W.; DiMagno, S. G.; Wang, C. H.; Therien, M. J. *J. Am. Chem. Soc.* **1996**, *118*, 1497.
(3) Large TPA cross-section values ($\sigma^{(2)} > 10^3$ GM) have been reported at around 800 nm in various porphyrin derivatives, using the femtosecond apertureless Z-scan method: (a) Ogawa, K.; Ohashi, A.; Kobuke, Y.; Kamada, K.; Ohta, K. *J. Am. Chem. Soc.* **2003**, *125*, 13356. (b) Drobizhev, M.; Stepanenko, Y.; Dzenis, Y.; Karotki, A.; Rebane, A.; Taylor, P. N.; Anderson, H. L. *J. Am. Chem. Soc.* **2004**, *126*, 15352. (c) Drobizhev, M.; Stepanenko, Y.; Dzenis, Y.; Karotki, A.; Rebane, A.; Taylor, P. N.; Anderson, H. L. *J. Phys. Chem. B* **2005**, *109*, 7223.
(4) The synthetic design of centrosymmetric molecules with large TPA cross-section values was investigated: Albota, M.; Beljonne, D.; Bredas, J.-L.; Ehrlich, J. E.; Fu, J.-Y.; Heikel, A. A.; Hess, S. E.; Kogej, T.; Levin, M. D.; Marder, S. R.; McCord-Maughon, D.; Perry, J. W.; Rockel, H.; Rumi, M.; Subramaniam, G.; Webb, W. W.; Wu, X.-L.; Xu, C. *Science* **1998**, *281*, 1653 and references are therein.
(5) (a) Neves, M. G. P. M. S.; Martins, R. M.; Tomé, A. C.; Silvestre, A. J. D.; Silva, A. M. S.; Félix, V.; Drew, M. G. B.; Cavaleiro, J. A. S. *Chem. Commun.* **1999**, 385. (b) Shin, J.-Y.; Furuta, H.; Yoza, K.; Igarashi, S.; Osuka, A. *J. Am. Chem. Soc.* **2001**, *123*, 7190. (c) Taniguchi, R.; Shimizu, S.; Suzuki, M.; Shin, J.-Y.; Furuta, H.; Osuka, A. *Tetrahedron Lett.* **2003**, *44*, 2505. (d) Suzuki, M.; Osuka, A. *Org. Lett.* **2003**, *5*, 3943.
(6) Studies on photphysical properties of expanded porphyrins are rather limited. (a) Levanon, H.; Regev, A.; Michaeli, S.; Galili, T.; Cyr, M.; Sessler, J. L. *Chem. Phys. Lett.* **1990**, *174*, 235. (b) Maiya, B. G.; Cyr, M.; Harriman, A.; Sessler, J. L. *J. Phys. Chem.* **1990**, *94*, 3597. (c) Guldi, D. M.; Mody, T. D.; Gerashimchuk, N. N.; Magda, D.; Sessler, J. L. *J. Am. Chem. Soc.* **2000**, *122*, 8289. (d) Shionoya, M.; Furuta, H.; Lynch, V.; Harriman, A.; Sessler, J. L. *J. Am. Chem. Soc.* **1992**, *114*, 5714.

 **10.1021/ja050895l CCC: $30.25** 

***Chart 1.*** Structures of Hexaphyrins(1.1.1.1.1.1)

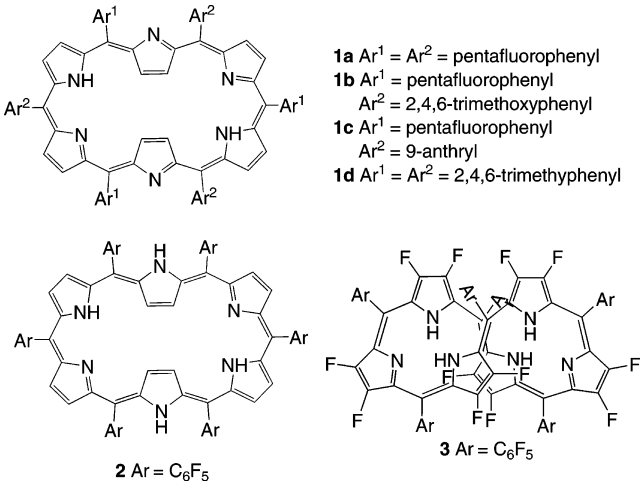


HOMO−LUMO gap, and rectangular molecular shape, hence possessing an important position bridging porphyrin and larger expanded porphyrins.[5a] Another useful character for the expanded $\pi$ conjugated molecular system is optical nonlinear properties such as two-photon absorption (TPA).

In this paper, we report comparative photophysical properties including excited singlet and triplet state dynamics and TPA cross-section values of *meso*-aryl substituted [26]- and [28]-hexaphyrins(1.1.1.1.1.1) using fluorescence lifetime, femtosecond transient absorption, nanosecond flash photolysis, and apertureless Z-scan measurements.[7] Overall, aromatic [26]-hexaphyrin gives a longer excited-state lifetime and larger TPA value than [28]hexaphyrin with antiaromaticity.

## Results and Discussion

**Photophysics of [26]Hexaphyrin(1.1.1.1.1.1).** The crystal structure of *meso*-hexakis(pentafluorophenyl) [26]hexaphyrin-(1.1.1.1.1.1) **1a** (Chart 1)[8] has a flat rectangular conformation with two inverted pyrrole rings, leading to the expected aromaticity of [4*n*+2] $\pi$ electrons. The absorption spectrum of **1a** shows a strong band at 568 nm, which presumably corresponds to the formally allowed Soret (B) band of porphyrins. Several low-energy bands at 712, 898, and 1026 nm may correspond to the weaker Q-bands of porphyrins (Figure 1). An increased conjugation of hexaphyrins is responsible for the large bathochromic shift and decreased HOMO−LUMO gap relative to porphyrins. The fluorescence of **1a** was measured with photoexcitation at 442 nm, whose spectrum shows the fluorescence maximum at 1036 nm with a weak vibronic band at 1205 nm (Figure 1). As compared to the absorption edge of 1026 nm, the Stokes shift is rather small (94 $cm^{-1}$), indicating a minimal structural change in the $S_1$ state relative to the ground state. The fluorescence quantum yield was roughly estimated to be less than $10^{-4}$. The fluorescence lifetime was measured by the time-correlated single-photon counting (TCSPC) technique, which yielded a lifetime of ~125 ps at 1030 nm upon photoexcitation at 405 nm (inset, Figure 1). It should be noted that this is much shorter than those of analogous molecules such as free-base porphyrin (~11.3 ns) and sapphyrin (~4.7 ns).[6d]

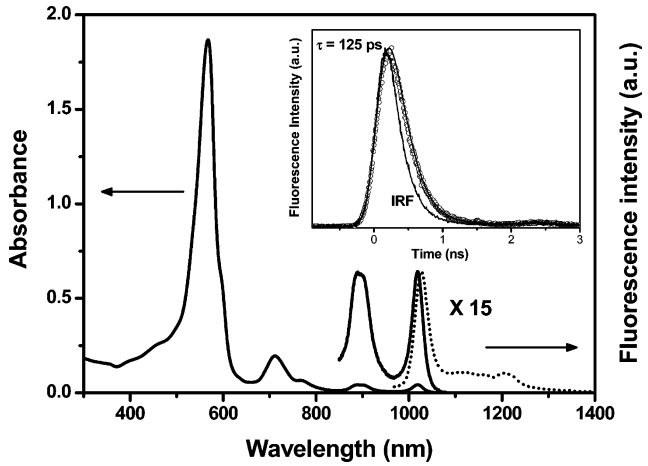


***Figure 1.*** Absorption and fluorescence spectra of **1a** in toluene. Inset shows a time-resolved fluorescence decay with $\tau$ = ~125 ps.

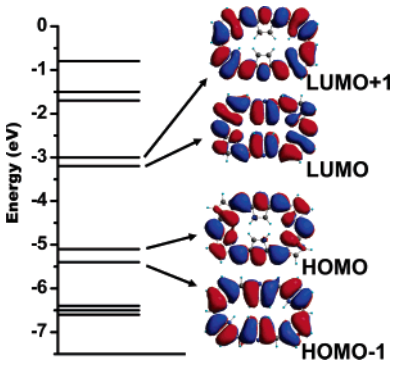


***Figure 2.*** Energy levels of frontier orbitals of [26]hexaphyrin from the geometry optimization process based on the ab initio calculation on B3LYP/6-31G level.

Ab initio calculations on the B3LYP/6-31G level were performed to examine the frontier orbitals as well as the optimized geometry (Figure 2). It is noteworthy that the overall features of the HOMO and LUMO of **1a** are, respectively, similar to the $a_{1u}$ and $a_{2u}$ HOMOs and two degenerate $e_g$* LUMOs of porphyrins, which explains the spectral resemblance between **1a** and porphyrin.[9]

The femtosecond transient absorption spectra of **1a** were recorded in the region of 400−1100 nm following photoexcitation at 400 nm in toluene. Aside from a rather featureless and broad induced absorption, strong ground-state bleaching was obtained (Figure 3). The decay profiles of bleaching and induced absorption at 570 and 640 nm, respectively, yielded a time constant of ~98 ps (inset, Figure 3), which is quite comparable to the fluorescence lifetime for the $S_1$ state lifetime.

To examine the excited triplet state dynamics, we carried out nanosecond flash photolysis for **1a** at 532 nm in toluene under an anaerobic condition (Figure 4). The T−T absorption spectrum recorded after photoexcitation is characterized by the $T_1$−$T_n$ absorption centered at 630 nm to the red side of the main bleaching band at 568 nm. The triplet state lifetime was measured at 530 and 640 nm, both of which yielded a lifetime of 1.8 $\mu$s at room temperature. Just as in fluorescence lifetime, the triplet state lifetime is significantly reduced for **1a** as compared to porphyrins. The quantum yield of triplet state formation was estimated to be $\Phi_{ISC}$ = 0.01 for **1a** using the

(7) Sheik-Bahae, M.; Said, A. A.; Wei, T.-H.; Hagan, D. G.; van Stryland, E. W. *IEEE J. Quantum Electron.* **1990**, *26*, 760.
(8) Preparation and compound data are given in refs 3b, 3d, and the Supporting Information.
(9) Chirvony, V. S.; Hoek, A.; Galievsky, V. A.; Sazanovich, I. V.; Schaafsma, T. J.; Holten, D. *J. Phys. Chem. B* **2000**, *104*, 9909.

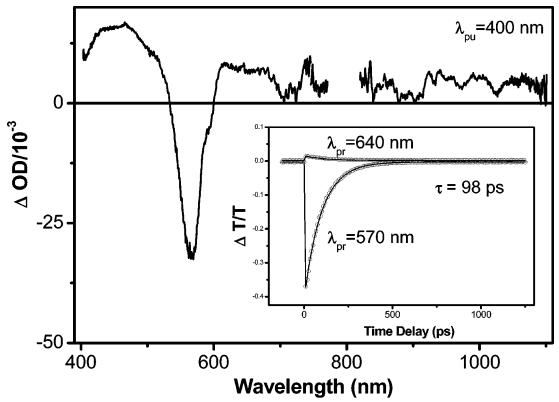


***Figure 3.*** Femtosecond transient absorption spectra of **1a** at zero time delay. Inset shows temporal decay curves at 570 and 640 nm for ground-state bleaching and induced absorption signals.

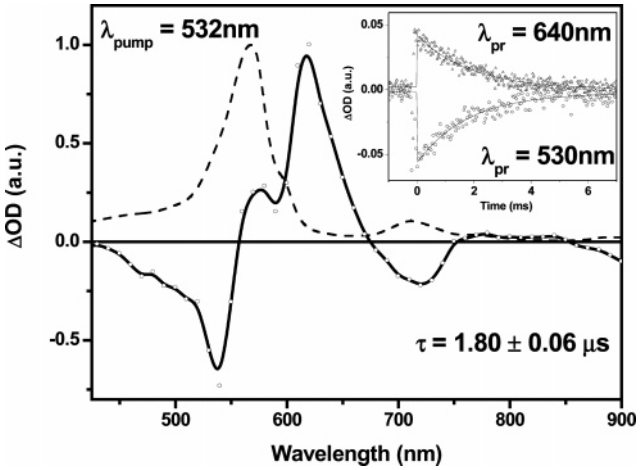


***Figure 4.*** Nanosecond flash photolysis spectra of **1a** in toluene under unaerobic conditions with photoexcitation at 532 nm. The triplet state lifetimes were measured at 530 and 640 nm for ground-state bleaching and induced absorption, respectively, which all give the lifetime of 1.8 $\mu$s at room temperature.

known value of $\Phi_{ISC} = 0.89$ for free-base porphyrin. Overall, the reduced HOMO−LUMO transition energy in **1a** dramatically enhances the internal conversion from the $S_1$ to the $S_0$ state with a very low quantum yield for triplet state formation.[10]

**Excited-State Dynamics of [28]Hexaphyrin(1.1.1.1.1.1).** It is known that **1a** undergoes reduction with $NaBH_4$ to produce *meso*-hexakis(pentafluorophenyl) [28]hexaphyrin(1.1.1.1.1.1) **2** with a vivid color change from violet to blue. The latter is easily converted to the former by oxidation with 2,3-dichloro-5,6-dicyano-1,4-benzoquinone (DDQ).[5] Although the solid-state crystal structure of **2** is unavailable, its conformation is conjectured to be a largely planar rectangular shape similar to **1a** as judged from the crystal structure of a related [28]-hexaphyrin molecule.[9] The $^1$H NMR spectra of **2** revealed no signal reflecting the anticipated antiaromatic ring current effect, which is presumably due to the slightly nonplanar geometry of **2** as compared to **1a**. The absorption spectrum for **2** exhibits a relatively broad Soret-like band with smeared Q-band-like transitions (Figure 5). Dual fluorescence bands with vibronic structures were observed at 1046 and 1210 nm with a relatively large Stokes shift of 290 cm$^{-1}$ (Figure 5). The ab initio calculation for **2** on the B3LYP/3-21G* level yielded a slightly

(10) Cho, H. S.; Ahn, T. K.; Yang, S. I.; Jin, S. M.; Kim, D.; Kim, S. K.; Kim, H. D. *Chem. Phys. Lett.* **2003**, *375*, 292.

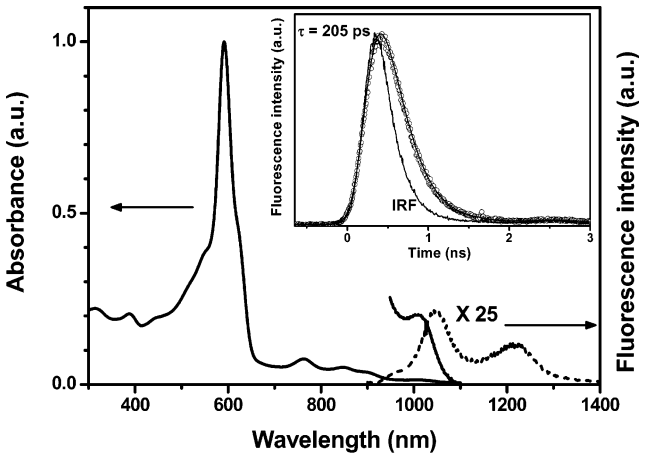


***Figure 5.*** Absorption and fluorescence spectra of **2** in toluene at room temperature. The inset shows time-resolved fluorescence decay profile at 1030 nm with photoexcitation at 405 nm. The decay profile was fitted by a deconvolution procedure with an IRF function, which gives ∼205 ps lifetime.

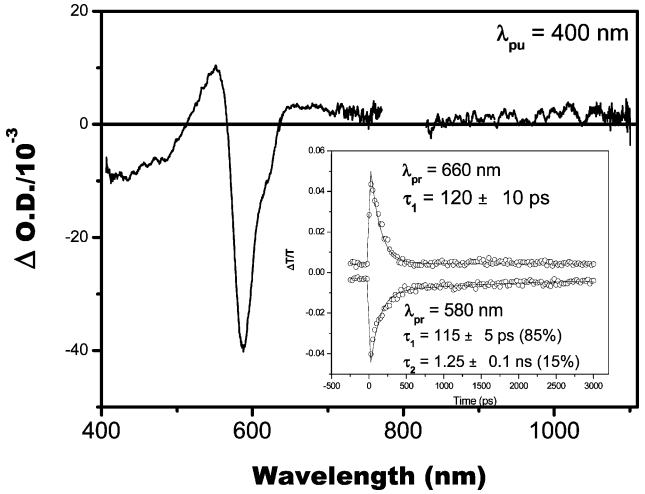


***Figure 6.*** Femtosecond transient absorption spectra of **2** in toluene at zero time delay with photoexcitation at 400 nm at 296 K. The inset shows temporal decay curves at 580 and 660 nm for induced absorption and ground-state bleaching, respectively, after photoexcitation at 400 nm. The dual decay times were estimated as 115 ± 5 ps and 1.25 ± 0.1 ns.

distorted nonplanar geometry, in contrast to the relatively flat structure for **1** (Supporting Information, Figure S1). The fluorescence lifetime of **2** revealed a lifetime of ∼205 ps at 1030 nm with excitation at 405 nm that is considerably longer than that of **1a** (inset, Figure 5).

The transient absorption decay profile of **2** at 570 nm exhibited a double exponential decay with time constants of ∼115 ps (85%) and 1.25 ns (15%) at 296 K (Figure 6). Because no signal was observed in nanosecond flash photolysis, the long decay component with the time constant of 1.2 ns may be assigned as an intersystem crossing. Considering these spectroscopic features of **2**, we suggest that the conformational dynamics may play an important role in the energy relaxation pathways as illustrated in the previous work by Chirvony et al. on the photophysical properties of free-base diacid porphyrins.[9] To check the possibility of conformational change in the excited state, we examined transient absorption decay kinetics of **2** by lowering the temperature to 273 K, which yielded the decreased time constants of ∼26 ps (72%) and 1.25 ns (28%).

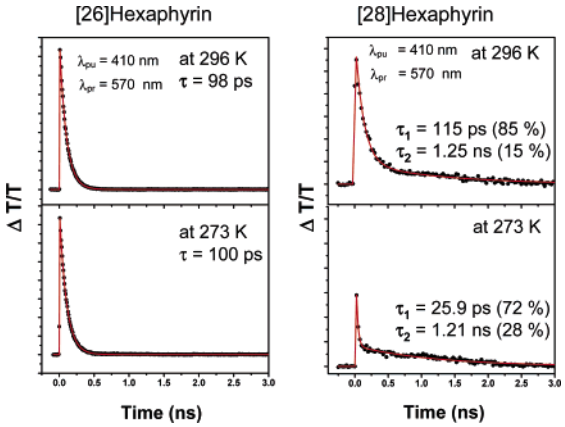


***Figure 7.*** The transient absorption decay profiles of **1a** and **2** at 570 nm at 296 and 273 K. Those of [28]hexaphyrin show exponential decays with time constants of ~115 ps (85%) and 1.25 ns (15%) at 296 K and ~26 ps (72%) and 1.25 ns (28%) at 273 K, which supports the conformational change in the excited state of **2**.

Free-base diacid porphyrins ($H_4TPP^{2+}$ and $H_4OEP^{2+}$) are known to exhibit nonplanar structural distortions relative to their corresponding neutral porphyrins ($H_2TPP$ and $H_2OEP$), which was confirmed by semiempirical PM3 calculations and X-ray crystallography.[9] As compared to neutral porphyrins, diacid porphyrins exhibit (1) spectral broadening in absorption and fluorescence spectra, (2) large Stokes shift, and (3) reduced excited-state lifetimes mainly due to their enhanced internal conversion ($S_1 \rightarrow S_0$) rates. In addition, $H_4TPP^{2+}$ was reported to experience a fluorescence lifetime change according to a change in temperature. They interpreted this temperature-dependent excited-state dynamics in terms of conformational change occurring in the excited state, which involves the activation process over the energy barrier leading to different nonradiative decay rates.[9] These features are quite similar to our spectroscopic observations on the excited-state dynamics of **2**. We also observed a slightly smaller Stokes shift in fluorescence emission at 273 K than at 296 K, supporting our interpretation of the conformational dynamics in the excited state of **2** (Supporting Information, Figure S2). On the contrary, the transient absorption decay of **1a** remains unchanged (~100 ps) with a change in temperature from 296 to 273 K, which precludes the possibility of conformational dynamics in the excited state of **1a** (Figure 7). Figure 8 presents a comparative schematic energy diagram based on our interpretations of the excited-state dynamics of **1a** and **2**.

**Two-Photon Absorption Behaviors of [26]- and [28]-Hexaphyrins(1.1.1.1.1.1).** There have been numerous research activities to search for new optical nonlinear materials with large two-photon absorption (TPA) cross sections ($\sigma^{(2)}$) due to potential applications in a variety of fields including photodynamic therapy, three-dimensional micro-fabrication and optical data storage, and optical limiting.[1] Among these, porphyrins with 18$\pi$-electronic system are quite promising, but high TPA performance has been achieved only when $\pi$-electronic networks are considerably enlarged either by conjugation with peripheral substituents and/or covalent and noncovalent assembling, because normal porphyrin monomers exhibit only small $\sigma^{(2)}$ values of less than $10^2$ GM.[2,3] We examined the TPA properties of **1** and **2** by an open-aperture Z-scan method (Supporting Information, Figure S3) with ~130 fs pulses at 1200 nm, and the results are summarized in Table 1. The TPA cross-section ($\sigma^{(2)}$) value

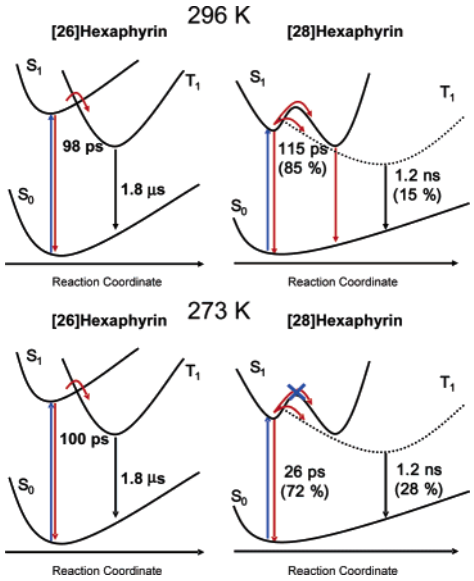


***Figure 8.*** Schematic diagrams of the excited states of **1a** and **2** to explain the temperature-dependent transient profiles. At 273 K, the excited-state conformer blocks the conformational change because of its energy barrier.

***Table 1.*** Absorption Band, TPA Cross Section, and $S_1$-State and $T_1$-State Lifetimes of Hexaphyrins(1.1.1.1.1.1)

| hexaphyrin | $\lambda_{max}$/nm | $\sigma^{(2)}$/GM | $\tau_S$/ps[f] | $\tau_T$/ns[g] |
|---|---|---|---|---|
| **1a** | 567,[a] 1018[b] | 9890 ± 230[d] | 98 | 1800 |
| **1b** | 574,[a] 1038[b] | 9490 ± 150[d] | 103 | 665 |
| **1c** | 574,[a] 1033[b] | 7790 ± 260[d] | 100 | —[h] |
| **1d** | 568,[a] 1038[b] | 7640 ± 190[d] | 101 | 52 |
| **2** | 594,[a] 1009[b,c] | 2600 ± 260[d] | 26 | —[h] |
| **3** | 498 | 810 ± 50[e] | 9.2 | —[h] |

[a] Soret-like absorption band. [b] Lowest energy Q-band-like absorption band. [c] Broad band. [d] Two-photon absorption cross-section ($\sigma^{(2)}$) value measured at 1200 nm. [e] $\sigma^{(2)}$ value measured at 800 nm. [f] $S_1$-state lifetime. [g] $T_1$-state lifetime. [h] No transient was observed by nanosecond flash photolysis.

of **1a** was measured to be 9890 GM at 1200 nm where the linear absorption is negligible (Supporting Information, Figure S4).[3,4,10] This value is much larger than those of porphyrin monomers by a factor of $>10^2$, being the largest among porphyrin-related monomeric pigments. Hexaphyrins **1b**, **1c**, and **1d** all exhibit large $\sigma^{(2)}$ values, 9490, 7790, and 7640 GM, respectively. The $^1$H NMR spectral data of **1b**−**1d** all indicate a strong diatropic ring current similar to **1a**. Therefore, it is concluded that the hexaphyrins **1a**−**1d** take the similar molecular shape and aromatic 26$\pi$-electronic system (Supporting Information, Figures S5−S7). Despite large and polarizable aromatic substituents such as 9-anthryl groups at the *meso*-positions (**1c**), the $\sigma^{(2)}$ values were not much influenced probably due to their tilting conformations against the hexaphyrin plane. Interestingly, the $S_1$-state lifetimes of **1a**−**1d** are nearly the same, ca. 100 ps, while their $T_1$-state lifetimes exhibit large variations depending on the *meso*-aryl substituents (Table 1).

In contrast, we observed the TPA value of 2600 GM for **2** at 1200 nm, which is consistent with the reduced aromaticity as compared to **1a**. Besides aromaticity determined by the number of $\pi$ electrons, the planarity of the hexaphyrin ring is likely to play an important role in maintaining the $\pi$ conjugation (Supporting Information, Figure S4). Furthermore, we measured the $\sigma^{(2)}$ value of perfluorinated *meso*-hexakis(pentafluorophenyl) [28]hexaphyrin(1.1.1.1.1.1) **3** that has a totally nonplanar figure

eight structure due to a lack of ring electron density, and its absorption spectrum exhibits a broad absorption band centered at 498 nm without any Q-band like low-energy absorption bands, and no fluorescence was detected,[13] hence featuring typical nonaromatic nature. The excited-state lifetime has been revealed quite short (9.2 ps) on the basis of the femtosecond transient absorption spectroscopy (Supporting Information, Figure S8). Interestingly, the $\sigma^{(2)}$ value of **3** was determined to be 810 GM at 800 nm, again reinforcing the dependence of the TPA absorption cross section on the aromaticity. Yet these results indicate that the extension of cyclic electronic network from porphyrin to hexaphyrin(1.1.1.1.1.1) leads to enhancement of $\sigma^{(2)}$ value even for the nonaromatic one. Thus, as the overall ring structure becomes planar in [26]hexaphyrins, a large TPA cross section is observed. It is noteworthy that the changes in the excited-state lifetimes for various [26]hexaphyrins are parallel with the increase of TPA cross-section values and the enhancement of ring planarity revealed by X-ray crystallography.

## Conclusion

In this work, we have revealed the overall dynamics of the $S_1$ and $T_1$-excited states of hexaphyrins **1**, **2**, and **3**, which constitute a useful platform for further investigations of the excited states of expanded porphyrins. Especially, we proved the conformational dynamics involved in the excited-state relaxation of **2** by temperature-dependent transient absorption decay measurements. In addition, large TPA cross sections (ca. $10^4$ GM) of the aromatic hexaphyrins **1** have been demonstrated, and their dependence on the aromaticity has been established. These large TPA cross sections of **1** are quite attractive and will be further enhanced by the extension of their $\pi$-electronic systems through suitable peripheral modification with conjugated substituents or covalent and/or noncovalent assembling.

## Experimental Section

**Sample Preparation.** The details of the synthesis of **1a**−**1d**, **2**, and **3** are described elsewhere[5,11] and in the Supporting Information. For example, in case of **1a**, a solution of methanesulfonic acid in $CH_2Cl_2$ (2.5 M, 12.5 mL) was added to a solution of pentafluorobenzaldehyde (0.5 mmol) and *meso*-pentafluorophenyl dipyrromethane (0.5 mmol) in dry $CH_2Cl_2$ (15 mL). The resulting solution was stirred for 2 h at 0 °C under nitrogen. After addition of 2,3-dichloro-5,6-dicyano-1,4-benzoquinone (DDQ, 500 mg), the solution was stirred for 3 h and passed through a short alumina column for neutralization and removal of tar with 10% methanol in $CH_2Cl_2$. After removal of the solvent by a rotary evaporator, the reaction mixture was separated by silica gel column chromatography with a mixture of $CH_2Cl_2$ and hexane (30:70) as an eluent.

**Near-IR Fluorescence Spectrum and Lifetime Measurements.** The fluorescence emission was detected using a near-IR photomultiplier (Hamamatsu, H9170-75), a lock-in amplifier (EG&G, 5210), combined with a chopper after laser excitation at 442 nm from a CW He−Cd laser (Melles Griot, Omnichrome 74). Time-resolved fluorescence was detected using a time-correlated single-photon-counting (TCSPC) technique.[14] As an excitation light source, we used a homemade cavity dumped Ti:Sapphire oscillator, which provided a high repetition rate (200−400 kHz) of ultrashort pulses (100 fs at full width half-maximum-(fwhm)) pumped by a CW Nd−$YVO_4$ laser (Spectra-Physics, Millennia). The output pulses of the oscillator were frequency-doubled with a second harmonic crystal. The TCSPC detection system consisted of near-IR photomultiplier (Hamamatsu, H9170-75), a TAC (EG&G Ortec, 457), two discriminators (EG&G Ortec, 584 (signal) and Canberra, 2126 (trigger)), and two wideband amplifiers (Philip Scientific (signal) and Mini Circuit (trigger)). A personal computer with a multichannel analyzer (Canberra, PCA3) was used for data storage and processing. The overall instrumental response function by an IR dye (Aldrich, IR1100) was about 410 ps (fwhm). For the deconvolution procedure, the IRF function was obtained by detecting emission from a IR dye molecule (Aldrich, IR1100) with a known lifetime of ~6 ps.

**Femtosecond Transient Absorption Measurements.** The dual-beam femtosecond time-resolved transient absorption spectrometer consisted of a self-mode-locked femtosecond Ti:sapphire laser (Coherent, MIRA), a Ti:sapphire regenerative amplifier (Clark MXR, CPA-1000) pumped by a Q-switched Nd:YAG laser (ORC-1000), a pulse stretcher/compressor, OPG-OPA system, and an optical detection system.[15] The pump beam was focused to a 1 mm diameter spot, and laser fluence was adjusted less than ~1.0 mJ $cm^{-2}$ by using a variable neutral-density filter. The fundamental beam remaining in the OPG-OPA system was focused onto a flowing water cell to generate white light continuum, which was again split into two parts. One part of the white light continuum was overlapped with the pump beam at the sample to probe the transient, while the other part of the beam was passed through the sample without overlapping the pump beam. The time delay between pump and probe beams was controlled by making the pump beam travel along a variable optical delay. The white continuum beams after sample were sent to a 15 cm focal length spectrograph (Acton Research) through each optical fiber and then detected by the dual 512 channel photodiode arrays (Princeton Instruments). The intensity of the white light of each 512 channel photodiode array was processed to calculate the absorption difference spectrum at the desired time delay between pump and probe pulses.

**Nanosecond Flash Photolysis Measurements.** The nanosecond transient absorption spectra were obtained by nanosecond flash photolysis technique.[16] An excitation pulse of 532 nm was generated from the second harmonic output of a Q-switched Nd:YAG laser (Continuum, Surelite). The time duration of the excitation pulse was ca. 6 ns, and the pulse energy was ca. 2 mJ/pulse. A CW Xe lamp (150 W) was used as a probe light source for transient absorption measurement. The probe light was collimated on the sample cell and then spectrally resolved by using a 15 cm monochromator (Acton Research, SP150) equipped with a 600 grooves/mm grating after passing the sample. The spectral resolution was about 3 nm for transient absorption experiment. The light signal was detected via a photomultiplier tube (Hamamatsu, R928). The output signal from the PMT was recorded with a 500 MHz digital storage oscilloscope (Tektronix, TDS3052) for the temporal profile measurement. Because the triplet state dynamics of molecules in solution is strongly dependent on the concentration of oxygen molecules dissolved in solution, we have tried to remove oxygen rigorously by repeated freeze pump thaw cycles. To ensure our data, we first examined the triplet state dynamics of Zn(II)TPP in toluene under unaerobic conditions, which gives about 1 ms lifetime at room temperature. Because the concentration of molecules also affects significantly the excited triplet state lifetime due to triplet−triplet annihilation processes, we have kept the concentration down to $10^{-5}$ M with relatively low photoexcitation density at 532 nm produced by the second harmonic output of a Q-switched Nd:YAG laser.

**Measurement of Two-Photon Absorption Cross Section ($\sigma^{(2)}$).** The TPA spectra were measured at 1200 nm by using the open-aperture

(11) Suzuki, M.; Shimizu, S.; Shin, J.-Y.; Osuka, A. *Tetrahedron Lett.* **2003**, *44*, 4597.
(12) Kim, D. Y.; Ahn, T. K.; Kwon, J. H.; Kim, D.; Ikeue, T.; Aratani, N.; Osuka, A.; Shigeiwa, M.; Maeda, S. *J. Phys. Chem. A* **2005**, *109*, 2996.
(13) Shimizu, S.; Shin, J.-Y.; Furuta, H.; Ismael, R.; Osuka, A. *Angew. Chem., Int. Ed.* **2003**, *42*, 78.
(14) Hwang, I.-W.; Cho, H. S.; Jeong, D. H.; Kim, D.; Tsuda, A.; Nakamura, T.; Osuka, A. *J. Phys. Chem. B* **2003**, *107*, 9977.
(15) Cho, H. S.; Song, N. W.; Kim, Y. H.; Jeoung, S. C.; Hahn, S.; Kim, D.; Kim, S. K.; Yoshida, N.; Osuka, A. *J. Phys. Chem. A* **2000**, *104*, 3287.
(16) Song, N. W.; Cho, H. S.; Yoon, M. C.; Aratani, N.; Osuka, A.; Kim, D. *Bull. Korean Chem. Soc.* **2002**, *23*, 271.

Z-scan method[7] with ~130 fs pulses from an optical parametric amplifier (Light Conversion, TOPAS) operating at 5 kHz repetition rate generated from a Ti:sapphire regenerative amplifier system (Spectra-Physics, Hurricane) (Figure S5). The laser beam was divided into two parts. One was monitored by a Ge/PN photodiode (New Focus) as intensity reference, and the other was used for transmittance measurement. After passing through an $f = 10$ cm lens, the laser beam was focused and passed through a quartz cell. The position of the sample cell could be varied along the laser-beam direction (*z*-axis), so the local power density within the sample cell could be changed under a constant laser power level. The thickness of the cell is 1 mm. The transmitted laser beam from the sample cell was then detected by the same photodiode as used for reference monitoring. The on-axis peak intensity of the incident pulses at the focal point, $I_0$, ranged from 40 to 60 GW $cm^{-2}$. Assuming a Gaussian beam profile, the nonlinear absorption coefficient $\beta$ can be obtained by curve fitting to the observed open-aperture traces with the following equation:[7]

$$T(z) = 1 - \frac{\beta I_0 (1 - e^{-\alpha_0 l})}{2\alpha_0 (1 + (z/z_0)^2)} \quad (1)$$

where $\alpha_0$ is the linear absorption coefficient, $l$ is the sample length, and $z_0$ is the diffraction length of the incident beam.

After obtaining the nonlinear absorption coefficient $\beta$, the TPA cross-section $\sigma^{(2)}$ of one solute molecule (in units of 1 GM = $cm^4$·s/photon·molecule) can be determined by using the following relationship:

$$\beta = \frac{\sigma^{(2)} N_A d \times 10^{-3}}{h\nu} \quad (2)$$

where $N_A$ is the Avogadro constant, $d$ is the concentration of the TPA compound in solution, $h$ is the Planck constant, and $\nu$ is the frequency of the incident laser beam.

We obtained the TPA cross-section $\sigma^{(2)}$ values of hexaphyrins at 1200 nm, where linear absorption is negligible, to satisfy the condition of $\alpha_0 l \ll 1$ in retrieving the pure TPA $\sigma^{(2)}$ values in the simulation procedure. We also measured the TPA cross-section value of AF-50 as a reference compound, which exhibits 50 GM at 800 nm.[17]

**Acknowledgment.** The work at Yonsei University was supported by the National Creative Research Initiatives Program of KOSEF. The work at Kyoto University was supported by the CREST of JST.

**Supporting Information Available:** Synthetic details (PDF); X-ray crystallographic data (CIF). This material is available free of charge via the Internet at http://pubs.acs.org.

JA050895L

(17) Kim, O. K.; Lee, K. S.; Woo, H. Y.; Kim, K. S.; He, G. S.; Swiatkiewicz, J.; Prasad, P. N. *Chem. Mater.* **2000**, *12*, 284.